Supplementary Material (ESI) for Journal of Materials Chemistry C
This journal is (c) The Royal Society of Chemistry 2013

Electronic Supplementary Information

Lanthanide-Doping Route to Aspect-Ratio-Controlled KSc_2F_7 Nanocrystals for Upconversion, Downconversion and Magnetism

Yujie Ding,[ab] Xiaoxia Zhang,[a] Hao Zhu[a] and Jun-Jie Zhu*[a]

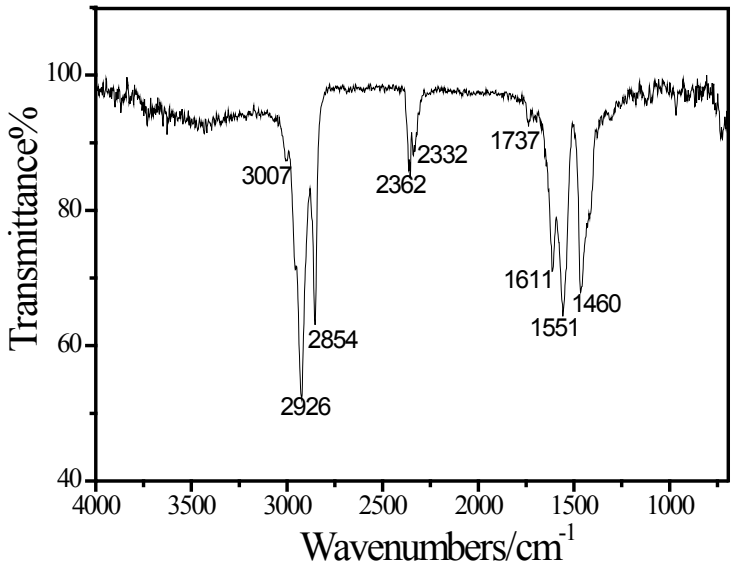

Fig. S1 FT-IR spectrum of the pure KSc_2F_7 NCs. As one can see, two peaks at 2926 cm^{-1} and 2854 cm^{-1} can be assigned to the asymmetric (ν_{as}) and symmetric (ν_s) stretching vibration of methylene (CH_2), respectively. In addition, the =C-H stretching mode is located at 3007 cm^{-1}. The weak absorption peak at 1737 cm^{-1} is attributed to C=O vibration frequency from the carboxyl of oleic acid. The peaks at 1551 cm^{-1} and 1460 cm^{-1} belong to the asymmetric (ν_{as}) and symmetric (ν_s) stretching vibration of the carboxylic group (-COOH), respectively. It can be concluded that the oleic acid is coordinated to the surface of KSc_2F_7 NCs.

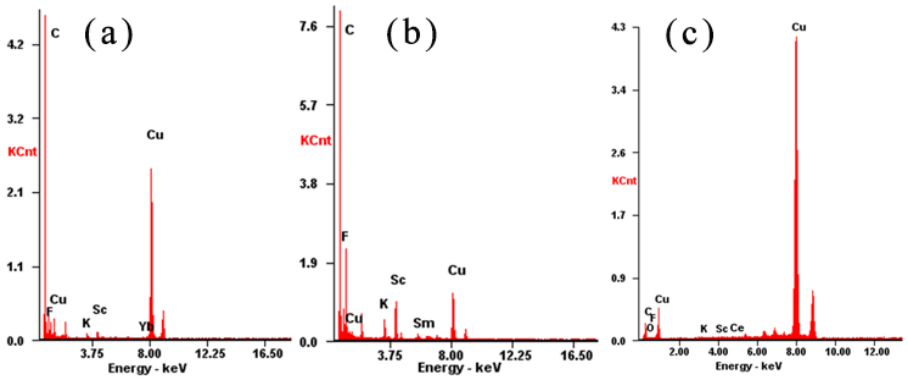

Fig. S2 EDS of (a) KSc_2F_7: 10% Yb^{3+}, (b) KSc_2F_7: 10% Sm^{3+}, (c) KSc_2F_7: 10% Ce^{3+}

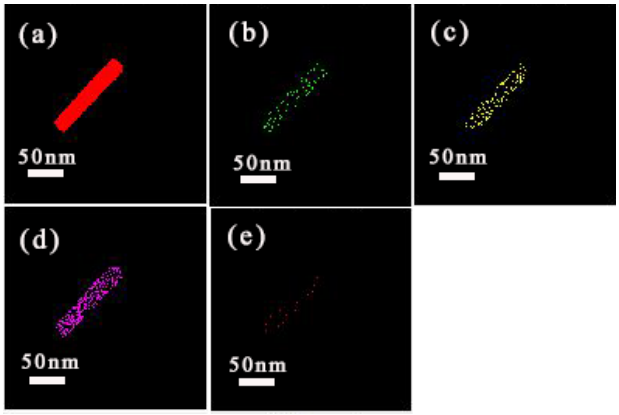

Fig. S3 STEM image of an individual nanorod of sample KSc_2F_7: 10% Yb^{3+} NCs (a) and the EDX element mapping of potassium (b), scandium (c), fluorine (d) and ytterbium (e).

Table S1 Compositions of the NCs measured by ICP-MS.

Sample	Initial doped [RE^{3+}] (at.%)	Doped [RE^{3+}] in NCs (at.%)
KSc_2F_7: 10% Lu^{3+}	10	8.58
KSc_2F_7: 10% Yb^{3+}	10	8.41
KSc_2F_7: 10% Dy^{3+}	10	9.03
KSc_2F_7: 10% Tb^{3+}	10	8.79
KSc_2F_7: 10% Eu^{3+}	10	9.32
KSc_2F_7: 10% Sm^{3+}	10	8.96
KSc_2F_7: 10% Ce^{3+}	10	8.65
KSc_2F_7: 10% La^{3+}	10	8.36
KSc_2F_7: 1% Sm^{3+}	1	0.92
KSc_2F_7: 5% Sm^{3+}	5	4.38
KSc_2F_7: 20% Sm^{3+}	20	16.87

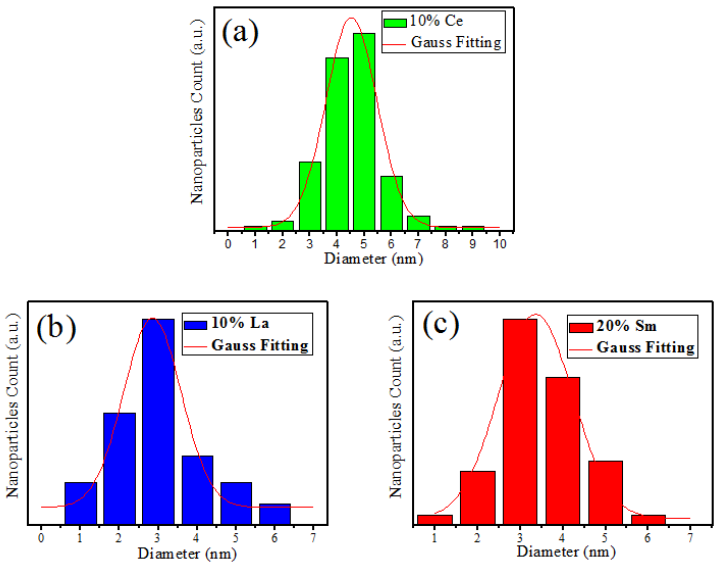

Fig. S4 Histograms of particle size for KSc_2F_7 doped with (a) 10% Ce^{3+}, (b) 10% La^{3+}, (c) 20% Sm^{3+}. These data were obtained from the TEM images of more than 300 KSc_2F_7 NCs. The average sizes for the NCs with 10% Ce^{3+}, 10% La^{3+} and 20% Sm^{3+} doping were found to be about 4.5 (with a standard deviation of 0.9), 3.8 (with a standard deviation of 0.8) and 3.4 (with a standard deviation of 0.9), respectively.

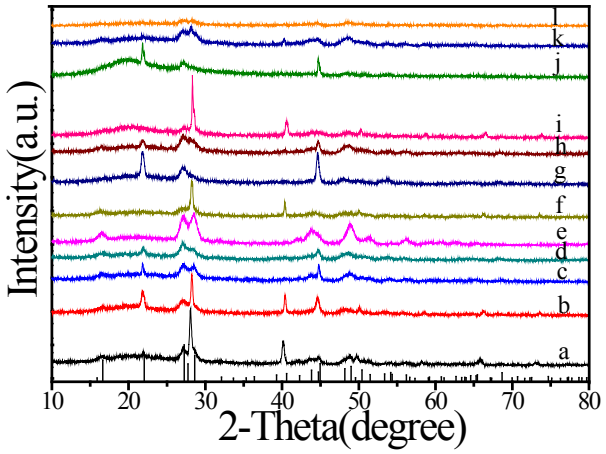

Fig. S5 XRD patterns of the KSc_2F_7 NCs. (a) KSc_2F_7: 1% Dy^{3+}, (b) KSc_2F_7: 5% Dy^{3+}, (c) KSc_2F_7: 10% Dy^{3+}, (d) KSc_2F_7: 20% Dy^{3+}, (e) KSc_2F_7: 1% Tb^{3+}, (f) KSc_2F_7: 5% Tb^{3+}, (g) KSc_2F_7: 10% Tb^{3+}, (h) KSc_2F_7: 20% Tb^{3+}, (i) KSc_2F_7: 1% Eu^{3+}, (j) KSc_2F_7: 5% Eu^{3+}, (k) KSc_2F_7: 10% Eu^{3+}, (l) KSc_2F_7: 20% Eu^{3+}. Line pattern (lower part) of the orthorhombic phase KSc_2F_7 (JCPDS card 77-1321).

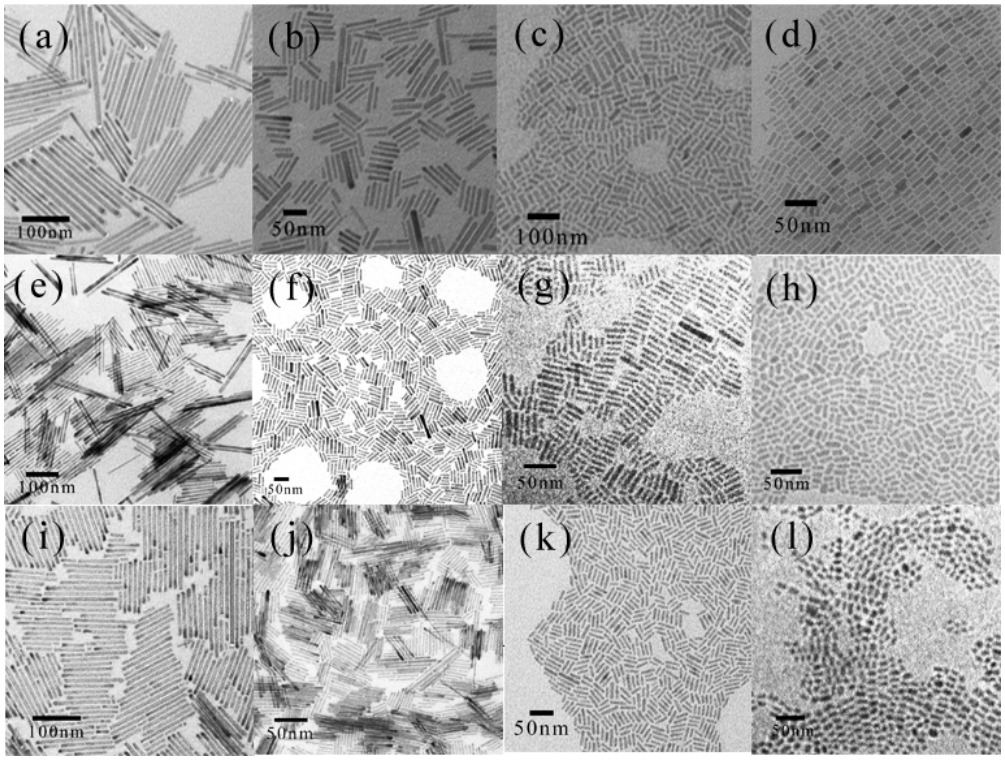

Fig. S6 TEM images of the KSc_2F_7 NCs. (a) KSc_2F_7: 1% Dy^{3+}, (b) KSc_2F_7: 5% Dy^{3+}, (c) KSc_2F_7: 10% Dy^{3+}, (d) KSc_2F_7: 20% Dy^{3+}, (e) KSc_2F_7: 1% Tb^{3+}, (f) KSc_2F_7: 5% Tb^{3+}, (g) KSc_2F_7: 10% Tb^{3+}, (h) KSc_2F_7: 20% Tb^{3+}, (i) KSc_2F_7: 1% Eu^{3+}, (j) KSc_2F_7: 5% Eu^{3+}, (k) KSc_2F_7: 10% Eu^{3+}, (l) KSc_2F_7: 20% Eu^{3+}.

Table S2 Length, diameter and aspect ratio from the TEM images in Fig. S6.

Dopants	Length (nm)	Diameter (nm)	Aspect Ratio	Dopants	Length (nm)	Diameter (nm)	Aspect Ratio
1% Dy^{3+}	140	6	23	20% Tb^{3+}	20	8	3
5% Dy^{3+}	62	7	9	1% Eu^{3+}	115	6	19
10% Dy^{3+}	57	12	5	5% Eu^{3+}	30	4	7
20% Dy^{3+}	22	6	4	10% Eu^{3+}	29	7	4
1% Tb^{3+}	123	6	21	20% Eu^{3+}	15	8	2
5% Tb^{3+}	48	7	7				
10% Tb^{3+}	35	7	5				

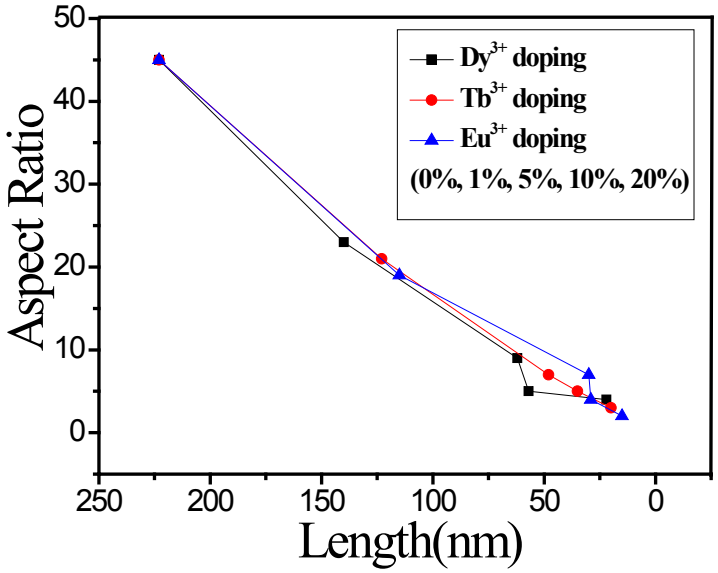

Fig. S7 Graph of aspect ratio versus length for RE^{3+}-doped KSc_2F_7 NCs (RE=Dy, Tb, Eu), the black dots are Dy^{3+}-doped KSc_2F_7 NCs, the red dots are Tb^{3+}-doped KSc_2F_7 NCs, the blue dots are Eu^{3+}-doped KSc_2F_7 NCs. (Each from left to right is 0%, 1%, 5%, 10% and 20% doping, respectively).

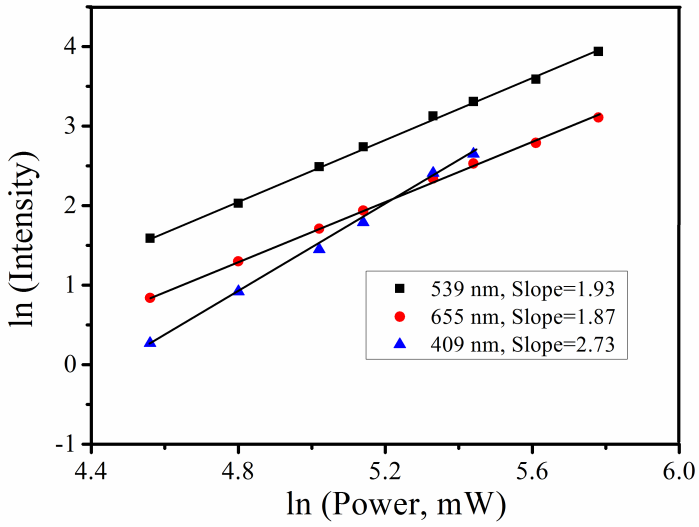

Fig. S8 Power dependence study of the UC emission of the KSc_2F_7: 10% Yb^{3+}, 1% Ho^{3+}, 10% Gd^{3+} NCs. Graph of ln (Intensity) versus ln (Power, mW) for the UC emission of Ho^{3+} is drawn. We can speculate that the 539 nm, 655 nm and 409 nm emissions of Ho^{3+} come from two-, two- and three-photon UC processes, respectively.

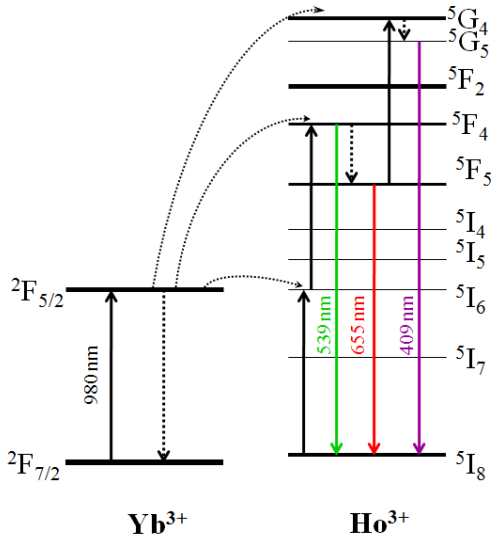

Fig. S9 Energy level diagram of Yb^{3+} ions and Ho^{3+} ions as well as UC emission mechanism in KSc_2F_7: 10% Yb^{3+}, 1% Ho^{3+}, 10% Gd^{3+} NCs. The excitation from the 980 nm laser is absorbed by Yb^{3+} ions, the electrons of Ho^{3+} ions are first excited from the $^5I_8$ ground-state to the $^5I_6$ level via excitation energy transfer from Yb^{3+} to Ho^{3+} ions, and then to the $^5F_4$ level by absorbing the energy of another electron from Yb^{3+} ions ($^2F_{5/2}$), hence, the green $^5F_4$ -$^5I_8$ emission (539 nm) occurs. The excited electrons of the $^5F_4$ (Ho^{3+}) level decay to the emitting $^5F_5$ level, mainly through nonradiative process, and the red $^5F_5 \rightarrow {}^5I_8$ emission (655 nm) occurs. The electrons of the Ho^{3+} in the $^5F_5$ excited state populate the $^5G_4$ level through a third 980 nm photon, and decay to the emitting $^5G_5$ level, leading to the purple emission of $^5G_5$–$^5I_8$ (409 nm).

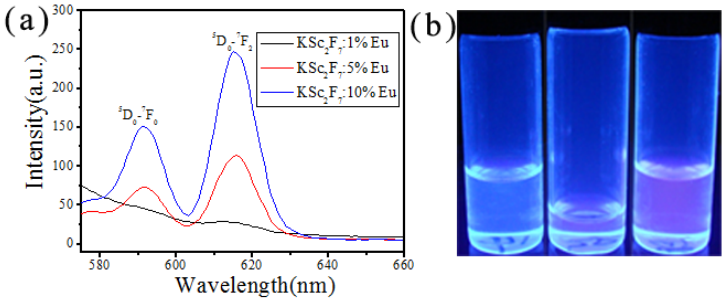

Fig. S10 (a) DC luminescence spectra of KSc_2F_7: x% Eu^{3+}. Black line is 1% Eu^{3+} doping, red line is 5% Eu^{3+} doping, blue line is 10% Eu^{3+} doping. (b) DC luminescence photography of KSc_2F_7: x% Eu^{3+} NCs under 265 nm excitation. One by one from left to right is 1% Eu^{3+}, 5% Eu^{3+}, 10% Eu^{3+}-doping, respectively.